Journal of Computational Applied Mechanics 2024, 55(2): 289-321

DOI: 10.22059/JCAMECH.2024.374370.1017

RESEARCH PAPER

Deflection, buckling and vibration analyses for a sandwich nanocomposite structure with foam core reinforced with GPLs and SMAs based on TSDBT

M. Arabzadeh-Ziari, M. Mohammadimehr *, E. Arabzadeh-Ziari, M. Asgari

Department of Solid Mechanics, Faculty of Mechanical Engineering, University of Kashan, Kashan, Iran P.O. Box 87317-53153.

Abstract

The purpose of this research is to investigate deflection, buckling and vibration for a five-layer sandwich nanocomposite beam, with reinforcements of graphene platelets (GPLs) and shape memory alloys (SMAs), and a foam core. To predict the behavior of the beam, theoretical formulations are derived based on the third order shear deformation beam theory (TSDBT). In order to check the validity and accuracy of the present work, the obtained results are compared with the results of other works and there is a good compatibility between them. It is concluded from this research that by using foam as the core, the weight of the structure is reduced, and also, the use of GPLs and SMAs as a reinforcement in the beam structure increases the stiffness and the equivalent elasticity modulus, so the ratio of strength to the weight of the structure increases. As a result of which the deflection decreases, the critical buckling load and the natural vibration frequencies of the beam increase. For example, it can be seen in the results that by increasing the volume fraction of GPL from 0 to 0.03, the deflection of the beam decreases by 44% and the first natural frequency of vibration and the critical buckling load increase by 31% and 79%, respectively.

Keywords: Sandwich nanocomposite structure; Foam core; GPL; SMA; Deflection, vibration and buckling.

1. Introduction

Nowadays, in the field of engineering, one of the main problems is the heavy weight of the structures, that's why sandwich composite structures have attracted a lot of attention among engineers and researchers due to their light weight and high hardness and strength. In compared to other materials, these structures have relative advantages in terms of better stability and corrosion resistance, longer fatigue life and higher strength-to-weight ratio. A sandwich composite structure generally consists of a light thick core and two stiff thin composite layers. These structures are used in various applications that require excellent mechanical properties with low weight, such as aerospace industries,

* *Corresponding author: Professor, Email: mmohammadimehr@kashanu.ac.ir*

satellites, automotive industries, marine transportation, civil, containers, tanks, body parts, rail cars, and wind energy systems [1-23].

In this field, some researches have been done to employ different materials as the core of sandwich and reinforcements for composite face sheets including carbon nanotubes (CNTs), graphene platelets and smart materials like shape memory alloys.

1.1. Employment of foam core

In the core of structures, materials with light weight such as polymer and metal foams are used, but its high thickness provides the structure with high flexural stiffness and low overall density. Kazemi [24] investigated the bending for a sandwich beam with aluminum face sheets and functionally graded (FG) polyurethane foam core. Alavinia and Kazemi [25] studied the ballistic resistance for a sandwich structures with aluminum face sheets and FG polyurethane foam core. Their analysis stated that with the increase in thickness and density of the foam, the ballistic limit and energy absorption increase. Qin and Wang [26] analyzed the large deflections for a thin sandwich beam with a metal foam core under lateral loading. Their study inspected that the structural response of sandwich beams depends on core strength, boundary conditions and punch size. Zhang et al. [27] checked the dynamic response and compressive strengths of sinusoidal sandwich plates without foam and filled with foam. Their investigation displayed that the use of foam-filled cores enhances the compressive strength, but does not have much effect on the dynamic response. Nasirzadeh and Sabet [28] inquired the influence of different densities for polyurethane foam core in a composite sandwich panel under impact loading. Their results demonstrated that foam with a density of 49 kg/m^3 has the best performance in terms of energy absorption.

1.2. Employment of graphene platelets

The effect of graphene platelets on strengthening the structure is such that the addition of a small amount of graphene can significantly improve the properties of the equivalent nanocomposite. This has prompted many researchers to study the behavior of graphene-reinforced nanocomposites and its derivatives. Feng et al. [29] considered the nonlinear vibration for a polymeric nanocomposite beam reinforced by GPLs. Their examination illustrated that the small use of GPLs in the polymer matrix has a significant reinforcing effect and can greatly increase frequencies of the beam. Wang et al. [30] regarded the nonlinear bending and vibration of GPLs reinforced composite beam with dielectric permittivity. Their analysis indicated that the thickness of the beam, the aspect ratio of the GPL and the electric voltage are very effective on bending and vibration of structure. Mohammadi et al [31] investigated the free vibration behavior of circular graphene face sheet and the effects of boundary conditions, mode number, small scale and preload on its natural frequencies. Their results showed that the effects of preloading are significant for the circular nanoplate with a smaller radius. Reddy et al. [32] depicted the free vibration of GPLs-reinforced multilayer composite plates, where the effect of parameters such as GPL distribution patterns, GPL weight fraction, edge boundary conditions, and GPL geometry on natural frequency are examined. Wu et al. [33] evaluated the dynamic instability of FG nanocomposite beams reinforced with GPLs. Numerical study presented that the natural frequency increases with more GPL distribution near the upper and lower surfaces, and GPL with a width-to-thickness ratio greater than 103 have a negligible effect. Kayani and Mirzaei [34] surveyed post-buckling and thermal buckling for composite beam reinforced with GPLs. According to their analysis, the critical buckling temperature increases significantly with FG distribution of GPL in the matrix. Mohammadi et al [35] studied the buckling of orthotropic monolayer graphene face sheets in thermal environment. They investigated the effects of temperature change, surrounding elastic environment and boundary conditions on the critical buckling load. It is determined that the small scale coefficient is highly effective on the critical buckling shear load of single-layer graphene face sheets. Song et al. [36] studied the vibration of randomly oriented GPL reinforced composite beams. They investigated the linear and nonlinear vibration of beams under the influence of different volume fractions and distribution patterns of GPL, GPL geometry and size, crack length and temperature changes. Feng et al. [37] checked nonlinear bending for a nanocomposite beam reinforced by non-uniformly distributed GPL. Yang et al. [38] analyzed post-buckling for a nanocomposite beams reinforced with low amount of GPLs. Their examination displayed that the post-buckling and buckling resistance of composite beams can be significantly increased by using GPLs. Wang et al. [39] researched the

vibration of a uniformly distributed GPL reinforced composite beam under two consecutive moving masses. Their analysis illustrated that adding a small amount of GPLs greatly increases beam stiffness and resistance to dynamic loads. Mohammadi et al. [40] analyzed the effect of temperature change, different boundary conditions, material properties and Winkler and Pasternak foundations on the vibration frequency of single-layer graphene face sheets, and it is concluded that increasing the temperature can reduce the non-dimensional frequency. Song et al. [41] presented bending and buckling studies of composite plate with FG-GPL. Their study showed that by adding a small amount of GPLs, the bending deflections decrease and the critical buckling load increases. Yang et al. [42] evaluated the nonlinear dynamic response of FG-GPL reinforced composite beams. They concluded that the GPL distribution is more effective when it is more at the top and bottom layers, and with this, dynamic deformation can be significantly reduced. Majidi et al. [43] surveyed the vibration of a composite sandwich plate surrounded by piezoelectric layers reinforced with GPLs. Their investigation indicated that the stiffness of the plate increases with the addition of a small amount of GPLs. Furthermore, the most effective reinforcement occurs by distributing more GPLs of larger size in the lower and upper surfaces of the plate. Mohammadi et al. [44] investigated the vibration behavior of annular and circular graphene face sheets. Their research findings showed that temperature change, boundary conditions and non-local parameters have significant effects on the vibration response.

1.3. Employment of shape memory alloys

SMAs constitute a group of metallic materials that have the ability to recover a predetermined length or shape when subjected to a thermodynamic process. The generated force and the change in the modulus of elasticity and density of the SMA modify the equivalent stiffness of the structure. As a result, SMA actuators can be used to control the displacement, vibration and buckling of composite structures. Li and Choi [45] regarded thermal buckling for a composite beam with SMA wires. Their analytical results inspected that thermal expansion is reduced by the recovery force, which increases the critical buckling temperature. Barzegari et al. [46] considered frequency and mode shape with SMA wires. According to their study, the frequency for the beam decreased with an increase in the number of SMA wires, at a temperature lower than the final temperature of martensite. Shiau et al. [47] examined the effect of SMA on the vibration of cross and angled layers under buckling by changing the spacing of SMA fibers. Their numerical examination stated that the stiffness of composite sheets increases with increasing of volume fraction of SMA fibers. In addition, the natural frequencies of the plate are modified. Park et al. [48] investigated the vibration of composite plate with SMA fibers. Their numerical study demonstrated that with the increase in the volume fraction and initial strain of SMA fiber, the stiffness of the plate increases. Kamarian et al [49] compared the performance of two advanced materials SMAs and CNTs in thermal buckling of composite beams. Their results expressed that the critical buckling temperature increases significantly by using both of these materials, but in some situations, the use of only one of SMAs or CNTs does not have much effect. Mahabadi et al. [50] presented the vibration response of SMAs reinforced composite plate. Asadi et al. [51] analyzed the vibration of composite hybrid beams with SMAHC in pre-buckling and post-buckling thermal domains. In the other work, they [52] studied the forced vibrations of a composite beam reinforced with SMA fibers (Nitinol). They concluded that the critical buckling temperature increases with the incorporation of SMA fibers and the recovery stress increases with the increase of SMA volume fraction.

1.4. Present work

The novelty of this research is the investigation of deflection, frequency and buckling simultaneously for a five-layer sandwich nanocomposite beam based on Reddy beam theory. Also, two types of nanoparticles, one from the family of smart materials (SMA) and the other with strengthening properties (GPL) are used in the beam structure along with other materials and their effects are obtained. The core is made of foam, the core face sheets are composed of a five-layer nanocomposite of carbon fibers and epoxy resin with graphene nanoplatelets reinforcements and the upper and lower layers of the beam are consists of epoxy resin with shape memory alloys. The results of this research show that by using reinforcements in the polymer matrix, high stiffness and modulus of elasticity can be achieved for the structure. It is also determined that the use of light cores such as foam reduces the weight of the structure, thus providing a high strength-to-weight ratio for the structure.

2. Material properties

The view of a five-layer sandwich nanocomposite beam with foam core, reinforced with GPLs and SMAs, is shown schematically in Fig 1. The displacement components of a sandwich nanocomposite beam are considered using the Cartesian coordinate system (x,y,z). Also, H_C, H_{GPL} and H_{SMA} are mentioned as the core thickness, the thickness of the nanocomposite face sheets with GPLs and the thickness of the layers with SMAs mixed in the resin, respectively.

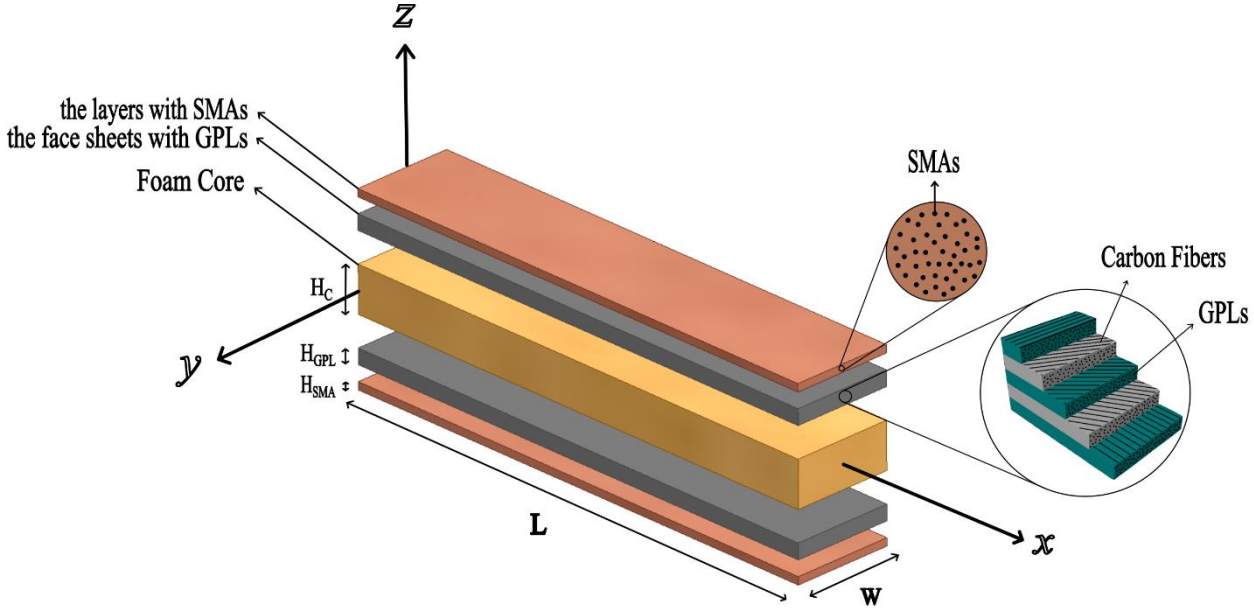

Fig 1. The schematic view of a five-layer sandwich nanocomposite beam with foam core, reinforced with GPLs and SMAs

Equivalent mechanical properties including modulus of elasticity, shear modulus, Poisson's ratio and density for nanocomposite layers that consist of carbon fibers, epoxy resin and graphene nanoplatelets are obtained based on the extended mixture rule. For this purpose, the equivalent properties of matrix are determined along with GPL reinforcements [53, 54].

$$E_{11\_mGPL} = \frac{\eta_1 \left(1+2(l_{GPL}/h_{GPL})\,\gamma_{11}\,V_{GPL}E_m\right)}{1-\gamma_{11}\,V_{GPL}}$$

$$E_{22\_mGPL} = \frac{\eta_2 \left(1+2(w_{GPL}/h_{GPL})\,\gamma_{22}\,V_{GPL}E_m\right)}{1-\gamma_{22}\,V_{GPL}} \qquad (1a)$$

$$G_{12\_mGPL} = \frac{\eta_3\, G_m}{1-\gamma_{12}\,V_{GPL}}$$

$$\nu_{12\_mGPL} = (\nu_{12\_GPL}\times V_{GPL}) + (\nu_m \times V_m)$$

$$\rho_{mGPL} = (\rho_{GPL}\times V_{GPL}) + (\rho_m \times V_m)$$

In which the values of γ coefficients are calculated as follows [55]:

$$\gamma_{11}=\frac{(E_{11\_GPL}/E_m)-1}{(E_{11\_GPL}/E_m)+2(l_{GPL}/h_{GPL})}$$
$$\gamma_{22}=\frac{(E_{22\_GPL}/E_m)-1}{(E_{22\_GPL}/E_m)+2(w_{GPL}/h_{GPL})} \quad (1b)$$
$$\gamma_{12}=\frac{(G_{12\_GPL}/G_m)-1}{(G_{12\_GPL}/G_m)}$$

In Eq. (1), E_{11_Gpl}, E_{22_Gpl}, G_{12_Gpl}, ρ_{GPL}, and υ_{12_GPL} are the modulus of elasticity, shear modulus, density and Poisson's ratio of GPL, respectively. The values of h_{GPL}, l_{GPL}, and w_{GPL} are related to the thickness, length, and width of GPL, respectively. The volume fraction of GPL and matrix are denoted by V_{GPL} and Vm, respectively. Also, the efficiency parameters indicated by η_1, η_2 and η_3, which depended on the volume fraction of GPL are obtained from Table 1 [56].

Table 1. The efficiency parameters (η_1, η_2 and η_3) according to volume fraction of GPL

V_{GPL}	η_1	η_2	η_3
0.03	2.929	2.855	11.842
0.07	3.013	2.966	23.575
0.11	2.311	2.260	32.125

Then, the total equivalent properties along with fibers are determined as follows [56]:

$$E_{11}=(E_{11\_mGPL}\times V_{mGPL})+(E_{11\_f}\times V_f)$$
$$E_{22}=\frac{1}{\left(\frac{V_{mGPL}}{E_{22\_mGPL}}+\frac{V_f}{E_{22\_f}}-V_fV_{mGPL}\times\left(\frac{\left(\nu_f^2E_{22\_mGPL}/E_{22\_f}\right)+\left(\nu_{12\_mGPL}^2E_{22\_f}/E_{22\_mGPL}\right)-2\nu_f\nu_{12\_mGPL}}{V_fE_{22\_f}+V_{mGPL}E_{22-mGPL}}\right)\right)} \quad (2)$$
$$G_{12}=\frac{1}{\left(\frac{V_{mGPL}}{G_{12\_mGPL}}+\frac{V_f}{G_{12\_f}}\right)}$$

$$\nu_{12}=(\nu_{12\_mGPL}\times V_{mGPL})+(\nu_f\times V_f)$$

$$\rho=(\rho_{mGPL}\times V_{mGPL})+(\rho_f\times V_f)$$

In Eq. (2), E_{11_f}, E_{22_f}, G_{12_f}, υ_f and ρ_f are the modulus of elasticity, shear modulus, Poisson's ratio and density of fibers, respectively. The volume fraction of fibers is displayed by V_f . V_{mGPL} is the sum of the volume fraction of matrix and GPL and is related to the volume fraction of fibers through the equation $V_{mGPL}=1-V_f$.

Equivalent mechanical properties of layers with SMAs are obtained using rules of mixture from the Eq. (3).

$$\begin{aligned} E &= (E_{SMA} \times V_{SMA}) + (E_m \times V_m) \\ G &= (G_{SMA} \times V_{SMA}) + (G_m \times V_m) \\ \upsilon &= (\upsilon_{SMA} \times V_{SMA}) + (\upsilon_m \times V_m) \\ \rho &= (\rho_{SMA} \times V_{SMA}) + (\rho_m \times V_m) \end{aligned} \tag{3}$$

The used mechanical properties in the beam structure are including foam, carbon fibers, epoxy resin, graphene platelets and shape memory alloys that are determined in Table 2 [56, 57].

Table 2. The values of mechanical properties of foam, carbon fibers, epoxy resin, graphene platelet and shape memory alloy (Nitinol)

Materials	Mechanical properties
Foam	$E = 0.1036$ GPa $G = 0.05$ GPa $\upsilon = 0.32$ $\rho = 130$ kg/m3
Carbon fibers	$E_{11\_f} = 233.05$ GPa , $E22\_f = 23.1$ GPa $G_{12\_f} = 8.96$ GPa $\upsilon_f = 0.2$ $\rho_f = 1750$ kg/m3
Epoxy resin	$E_m = 15.47$ GPa $G_m = 5.931$ GPa $\upsilon_m = 0.34$ $\rho_m = 1100$ kg/m3
Graphene platelet	$E_{11\_Gpl} = 1812$ GPa , $E_{22\_Gpl} = 1807$ GPa $G_{12\_Gpl} = 683$ GPa $\upsilon_{12\_GPL} = 0.177$ $\rho_{GPL} = 4118$ kg/m3 $l_{GPL}=14.76$ nm , $h_{GPL}=0.188$ nm , $w_{GPL}=14.77$ nm
Shape memory alloy (Nitinol)	$E_A = 67$ GPa , $E_M = 26.3$ GPa $G_M = 9.8872$ GPa $\upsilon = 0.33$ $\rho = 6450$ kg/m3

The working temperature of the problem is assumed ambient temperature and only the martensite phase of SMAs is considered, that is: $E_{SMA}=E_M=26.3$ GPa.

3. Theoretical formulation

The displacement fields based on the third order shear deformation beam theory (TSDBT) for the sandwich nanocomposite beam are written as follows [58, 59]:

$$\begin{cases} U(x,y,z,t) = u(x,t) + z\left(\psi(x,t) - \frac{4}{3}(\frac{z^2}{H^2})\left(\psi(x,t) + \frac{\partial w(x,t)}{\partial x}\right)\right) \\ V(x,y,z,t) = 0 \\ W(x,y,z,t) = w(x,t) \end{cases} \tag{4}$$

where W, U, V are the transverse and axial displacements, and also w, u, v are the transverse and axial displacements at the middle plane [60], ψ is the rotation of the cross section of the beam. Also, the strain components are obtained using equations of strain-displacement and Eq. (4) as follows:

$$\begin{aligned} \varepsilon_x &= \frac{\partial U}{\partial x} = (\frac{\partial u}{\partial x}) + z(\frac{\partial \psi}{\partial x}) - \frac{4z^3}{3H^2}(\frac{\partial \psi}{\partial x}) - \frac{4z^3}{3H^2}(\frac{\partial^2 w}{\partial x^2}) \\ \varepsilon_y &= \frac{\partial V}{\partial y} = 0 \\ \varepsilon_z &= \frac{\partial W}{\partial z} = 0 \\ \gamma_{xy} &= \frac{\partial U}{\partial y} + \frac{\partial V}{\partial x} = 0 \\ \gamma_{yz} &= \frac{\partial V}{\partial z} + \frac{\partial W}{\partial y} = 0 \\ \gamma_{xz} &= \frac{\partial U}{\partial z} + \frac{\partial W}{\partial x} = (\psi + \frac{\partial w}{\partial x})(1 - 4(\frac{z}{H})^2) \end{aligned} \tag{5}$$

In Eq. (5), normal and shear strains in different directions are represented by ϵ and γ, respectively. The governing equations of a sandwich beam is obtained by the following equation [61, 62]:

$$\int_{t_1}^{t_2} (\delta T - \delta U - \delta W_{ext})\, dt = 0 \tag{6}$$

where T, U and W_{ext} are kinetic energy, strain energy and energy caused by external forces acting on the beam, respectively. The strain energy variation for the sandwich nanocomposite beam and using Eq. (5) is written as follows [63]:

$$
\begin{aligned}
U &= \frac{1}{2}\int (\sigma_{ij}\varepsilon_{ij} + \tau_{ij}\gamma_{ij})dV \\
\delta U &= \int (\sigma_x \delta\varepsilon_x + \tau_{xz}\delta\gamma_{xz})\, dV \\
\delta U &= -\int \left(\begin{array}{l} \dfrac{\partial N_x}{\partial x}\delta u + \dfrac{\partial M_x^{(1)}}{\partial x}\delta\psi - \dfrac{4}{3H^2}\dfrac{\partial M_x^{(3)}}{\partial x}\delta\psi + \dfrac{4}{3H^2}\dfrac{\partial^2 M_x^{(3)}}{\partial x^2}\delta w \\ -Q_x\delta\psi + \dfrac{4}{H^2}M_{xz}^{(2)}\delta\psi - \dfrac{4}{H^2}\dfrac{M_{xz}^{(2)}}{\partial x}\delta w + \dfrac{\partial Q_x}{\partial x}\delta w \end{array} \right) dA
\end{aligned}
\tag{7}
$$

where [64, 65]:

$$
\begin{aligned}
N_x &= \int \sigma_x \, dz \\
M_x^{(i)} &= \int \sigma_x z^{(i)} \, dz \quad , \; i = 1,3 \\
Q_x &= \int \tau_{xz} \, dz \\
M_{xz}^{(2)} &= \int \tau_{xz} z^{(2)} \, dz
\end{aligned}
\tag{8}
$$

The variation of the external work for the sandwich nanocomposite beam is obtained as follows:

$$
\begin{aligned}
W_{ext} &= -\frac{1}{2}\int \left(q_{(x)}w + H_{(x)}u + P_{cr}(\frac{\partial w}{\partial x})^2 \right) dA \\
\delta W_{ext} &= -\int \left(q_{(x,t)}\delta w + H_{(x,t)}\delta u - P_{cr}\frac{\partial^2 w}{\partial x^2}\delta w \right) dA
\end{aligned}
\tag{9}
$$

The kinetic energy variation for the sandwich nanocomposite beam using Eq. (4) is obtained as follows:

$$T = \frac{1}{2}\int \rho(\dot{U}^2 + \dot{V}^2 + \dot{W}^2)\mathrm{dV}$$

$$\delta T = \int \rho(\frac{\partial U}{\partial t}\delta\frac{\partial U}{\partial t} + \frac{\partial V}{\partial t}\delta\frac{\partial V}{\partial t} + \frac{\partial W}{\partial t}\delta\frac{\partial W}{\partial t})\, dV$$

$$\delta T = \int \left(\begin{array}{l} I^{(0)}(-\frac{\partial^2 u}{\partial t^2}\delta u - \frac{\partial^2 w}{\partial t^2}\delta w) + I^{(1)}(-\frac{\partial^2 u}{\partial t^2}\delta\psi - \frac{\partial^2 \psi}{\partial t^2}\delta u) + I^{(2)}(-\frac{\partial^2 \psi}{\partial t^2}\delta\psi) \\ -\frac{4I^{(3)}}{3H^2}(-\frac{\partial^2 u}{\partial t^2}\delta\psi + \frac{\partial^3 u}{\partial x\,\partial t^2}\delta w - \frac{\partial^2 \psi}{\partial t^2}\delta u - \frac{\partial^3 w}{\partial x\,\partial t^2}\delta u) \\ -\frac{4I^{(4)}}{3H^2}(-\frac{\partial^2 \psi}{\partial t^2}\delta\psi + \frac{\partial^3 \psi}{\partial x\,\partial t^2}\delta w - \frac{\partial^2 \psi}{\partial t^2}\delta\psi - \frac{\partial^3 w}{\partial x\,\partial t^2}\delta\psi) \\ +\frac{16I^{(6)}}{9H^4}(-\frac{\partial^2 \psi}{\partial t^2}\delta\psi + \frac{\partial^3 \psi}{\partial x\,\partial t^2}\delta w - \frac{\partial^3 w}{\partial x\,\partial t^2}\delta\psi + \frac{\partial^4 w}{\partial x^2\partial t^2}\delta w) \end{array} \right) dA \quad (10)$$

where:

$$I^{(i)} = \int \rho z^{(i)}\, dz \quad , \quad i = 0,1,2,3,4,6 \quad (1)$$

Based on the Eqs. (7), (9) and (10), the equations of motion for the sandwich nanocomposite beam are written as follows [66, 67]:

$$\delta u \to H_{(x,t)} = \begin{pmatrix} I^{(0)}\frac{\partial^2 u}{\partial t^2} + I^{(1)}\frac{\partial^2 \psi}{\partial t^2} - \frac{4I^{(3)}}{3H^2}(\frac{\partial^2 \psi}{\partial t^2} + \frac{\partial^3 w}{\partial x \partial t^2}) - A^{(0)}u'' - A^{(1)}\psi'' \\ + \frac{4A^{(3)}}{3H^2}\psi'' + \frac{4A^{(3)}}{3H^2}w''' \end{pmatrix}$$

$$\delta w \to q_{(x,t)} = \begin{pmatrix} I^{(0)}\frac{\partial^2 w}{\partial t^2} + \frac{4I^{(3)}}{3H^2}\frac{\partial^3 u}{\partial x \partial t^2} + \frac{4I^{(4)}}{3H^2}\frac{\partial^3 \psi}{\partial x \partial t^2} - \frac{16I^{(6)}}{9H^4}\frac{\partial^3 \psi}{\partial x \partial t^2} - \frac{16I^{(6)}}{9H^4}\frac{\partial^4 w}{\partial x^2 \partial t^2} \\ -\frac{4}{3H^2}(A^{(3)}u''' + A^{(4)}\psi''' - \frac{4A^{(6)}}{3H^2}\psi''' - \frac{4A^{(6)}}{3H^2}w''') \\ +\frac{4}{H^2}(B^{(2)}\psi' - \frac{4B^{(4)}}{H^2}\psi' - \frac{4B^{(4)}}{H^2}w'' + B^{(2)}w'') \\ -B^{(0)}\psi' + \frac{4B^{(2)}}{H^2}\psi' + \frac{4B^{(2)}}{H^2}w'' - B^{(0)}w'' + P_{cr}w'' \end{pmatrix} \quad (12)$$

$$\delta\psi \to \begin{pmatrix} I^{(1)}\frac{\partial^2 u}{\partial t^2} + I^{(2)}\frac{\partial^2 \psi}{\partial t^2} - \frac{4I^{(3)}}{3H^2}\frac{\partial^2 u}{\partial t^2} - \frac{8I^{(4)}}{3H^2}\frac{\partial^2 \psi}{\partial t^2} - \frac{4I^{(4)}}{3H^2}\frac{\partial^3 w}{\partial x \partial t^2} \\ +\frac{16I^{(6)}}{9H^4}\frac{\partial^2 \psi}{\partial t^2} + \frac{16I^{(6)}}{9H^4}\frac{\partial^3 w}{\partial x \partial t^2} \\ -A^{(1)}u'' - A^{(2)}\psi'' + \frac{4A^{(4)}}{3H^2}\psi'' + \frac{4A^{(4)}}{3H^2}w''' \\ +\frac{4}{3H^2}(A^{(3)}u'' + A^{(4)}\psi'' - \frac{4A^{(6)}}{3H^2}\psi'' - \frac{4A^{(6)}}{3H^2}w''') \\ +B^{(0)}\psi - \frac{4B^{(2)}}{H^2}\psi - \frac{4B^{(2)}}{H^2}w' + B^{(0)}w' \\ -\frac{4}{H^2}(B^{(2)}\psi - \frac{4B^{(4)}}{H^2}\psi - \frac{4B^{(4)}}{H^2}w' + B^{(2)}w') \end{pmatrix} = 0$$

where:

$$A^{(i)} = \int E z^{(i)}\, dz \quad , \quad i = 0,1,2,3,4,6$$
$$B^{(i)} = \int G z^{(i)}\, dz \quad , \quad i = 0,2,4 \quad (2)$$

Considering the simple supported boundary conditions for a sandwich beam, Navier's solution method is used to find the stiffness and mass matrix [68], where the forces and displacements are estimated as the following functions:

$$
\begin{aligned}
H(x,t) &= \sum H_m \cos\left(\frac{m\pi x}{L}\right) e^{i\omega t} \\
q(x,t) &= \sum q_m \sin\left(\frac{m\pi x}{L}\right) e^{i\omega t} \\
u(x,t) &= \sum u_m \cos\left(\frac{m\pi x}{L}\right) e^{i\omega t} \\
w(x,t) &= \sum w_m \sin\left(\frac{m\pi x}{L}\right) e^{i\omega t} \\
\psi(x,t) &= \sum \psi_m \cos\left(\frac{m\pi x}{L}\right) e^{i\omega t}
\end{aligned}
\tag{14}
$$

Using equations of motion and Navier's solution method, three equations are obtained in terms of u_m, w_m, and ψ_m, and the matrix [R] is formed as follows:

$$
\left.
\begin{aligned}
[\Delta] &= \begin{bmatrix} u_m \\ w_m \\ \psi_m \end{bmatrix} \\
[\mathrm{F}] &= \begin{bmatrix} H_m \\ q_m \\ 0 \end{bmatrix}
\end{aligned}
\right\} \rightarrow [\mathrm{R}][\Delta] = [\mathrm{F}]
\tag{15}
$$

Now, each of the flexural stiffness, geometric stiffness and mass matrices are separated from the total matrix. Flexural stiffness matrix:

$$\left[K\right]=\begin{bmatrix} K_{11} & K_{12} & K_{13} \\ K_{21} & K_{22} & K_{23} \\ K_{31} & K_{32} & K_{33} \end{bmatrix}$$

$$K_{11}=(A^{(0)})(\frac{m\pi}{L})^2$$

$$K_{12}=(-\frac{4A^{(3)}}{3H^2})(\frac{m\pi}{L})^3$$

$$K_{13}=(A^{(1)})(\frac{m\pi}{L})^2-(\frac{4A^{(3)}}{3H^2})(\frac{m\pi}{L})^2$$

$$K_{21}=(-\frac{4A^{(3)}}{3H^2})(\frac{m\pi}{L})^3$$

$$K_{22}=(\frac{16A^{(6)}}{9H^4})(\frac{m\pi}{L})^4+(\frac{16B^{(4)}}{H^4})(\frac{m\pi}{L})^2-(\frac{8B^{(2)}}{H^2})(\frac{m\pi}{L})^2+(B^{(0)})(\frac{m\pi}{L})^2$$

$$K_{23}=(-\frac{4A^{(4)}}{3H^2})(\frac{m\pi}{L})^3+(\frac{16A^{(6)}}{9H^4})(\frac{m\pi}{L})^3-(\frac{8B^{(2)}}{H^2})(\frac{m\pi}{L})+(\frac{16B^{(4)}}{H^4})(\frac{m\pi}{L})+(B^{(0)})(\frac{m\pi}{L})$$

$$K_{31}=(A^{(1)})(\frac{m\pi}{L})^2-(\frac{4A^{(3)}}{3H^2})(\frac{m\pi}{L})^2$$

$$K_{32}=(-\frac{4A^{(4)}}{3H^2})(\frac{m\pi}{L})^3+(\frac{16A^{(6)}}{9H^4})(\frac{m\pi}{L})^3-(\frac{8B^{(2)}}{H^2})(\frac{m\pi}{L})+(\frac{16B^{(4)}}{H^4})(\frac{m\pi}{L})+(B^{(0)})(\frac{m\pi}{L})$$

$$K_{33}=(A^{(2)})(\frac{m\pi}{L})^2-(\frac{8A^{(4)}}{3H^2})(\frac{m\pi}{L})^2+(\frac{16A^{(6)}}{9H^4})(\frac{m\pi}{L})^2+(B^{(0)})-(\frac{8B^{(2)}}{H^2})+(\frac{16B^{(4)}}{H^4}) \quad (16)$$

Geometric stiffness matrix:

$$\left[K_P\right]=\begin{bmatrix} 0 & 0 & 0 \\ 0 & -P_{cr}(\frac{m\pi}{L})^2 & 0 \\ 0 & 0 & 0 \end{bmatrix} \quad (17)$$

Mass matrix:

$$\left[M\right]=\begin{bmatrix} M_{11} & M_{12} & M_{13} \\ M_{21} & M_{22} & M_{23} \\ M_{31} & M_{32} & M_{33} \end{bmatrix}$$

$$\begin{aligned}
M_{11} &= (I^{(0)}) \\
M_{12} &= (-\frac{4I^{(3)}}{3H^2})(\frac{m\pi}{L}) \\
M_{13} &= (I^{(1)}) - (\frac{4I^{(3)}}{3H^2}) \\
M_{21} &= (-\frac{4I^{(3)}}{3H^2})(\frac{m\pi}{L}) \\
M_{22} &= (I^{(0)}) + (\frac{16I^{(6)}}{9H^4})(\frac{m\pi}{L})^2 \\
M_{23} &= (-\frac{4I^{(4)}}{3H^2})(\frac{m\pi}{L}) + (\frac{16I^{(6)}}{9H^4})(\frac{m\pi}{L}) \\
M_{31} &= (I^{(1)}) - (\frac{4I^{(3)}}{3H^2}) \\
M_{32} &= (-\frac{4I^{(4)}}{3H^2})(\frac{m\pi}{L}) + (\frac{16I^{(6)}}{9H^4})(\frac{m\pi}{L}) \\
M_{33} &= (I^{(2)}) - (\frac{8I^{(4)}}{3H^2}) + (\frac{16I^{(6)}}{9H^4});
\end{aligned} \tag{18}$$

The deflection of the sandwich nanocomposite beam is calculated using the [K] and [F] matrices from the following equation:

$$\left[K\right]\begin{bmatrix} u_m \\ w_m \\ \psi_m \end{bmatrix}=\left[\mathrm{F}\right] \rightarrow \begin{bmatrix} u_m \\ w_m \\ \psi_m \end{bmatrix}=\left[K\right]^{-1}\left[\mathrm{F}\right] \tag{19}$$

The natural frequencies of the beam are obtained using the [K] and [M] matrices from the following equation [69, 70]:

$$\det\left(\left[K\right]-\omega^2\left[M\right]\right)=0 \tag{20}$$

The critical buckling load of the beam is obtained by using the [K] and [K_P] matrices and the determinants of the sum of these two matrices:

$$\det\left(\left[K\right]+\left[K_P\right]\right)=0 \tag{21}$$

4. Validation

In this section, the validation and verification of the accuracy of the solution method for this research is investigated. For this purpose, the obtained dimensionless fundamental natural frequency and the dimensionless critical buckling load from the present study are compared with the results of other studies and the results state a satisfactory agreement between them. The dimensionless frequency is compared to the results of Santos and Reddy [71] in Table 3 and Koochaki [72], Akhavan Alavi et al. [58] in Table 4 and the error percentage is determined.

It is noted that to validate Table 4, Eq. (13) must be modified as follows:

$$A^{(i)}=\int\frac{E}{1-\upsilon^2}z^{(i)}\,dz \quad , \quad i=0,1,2,3,4,6$$
$$B^{(i)}=\int Gz^{(i)}\,dz \quad , \quad i=0,2,4 \tag{22}$$

Also, the dimensionless parameter of frequency should be defined as follows:

$$(\overline{\omega}=\omega(\frac{L^2}{H})\sqrt{\frac{\rho_c}{E_c}}) \tag{23}$$

so, with these corrections in the code, the maximum error percentage was 0.12.

In Table 3, it is shown that with increasing aspect ratio (L/H), the error percentage decreases, because it trends to the slender beam. Also, in Table 4, with an increase in H/L, the error percentage enhances.

$$(\overline{\omega} = \omega L^2 \sqrt{\frac{I^{(0)}}{EI}})$$

Table 3. The nondimensional fundamental natural frequency of a sandwich nanocomposite beam

L/H	Santos and Reddy [71]	present study	Error %
5	9.3990	9.2745	1.34
10	9.7454	9.7075	0.39
20	9.8381	9.8281	0.10

$$(\overline{\omega} = \omega(\frac{L^2}{H})\sqrt{\frac{\rho_c}{E_c}})$$

Table 4. The dimensionless fundamental natural frequency of a functionally graded beam(k=0)

H/L	Koochaki [72]	AkhavanAlavi et al. [58]	present study	Error1 %	Error2%
0.01	2.9861380	2.9861344	2.9861723	0.00115	0.00127
0.0125	2.9858280	2.9858287	2.9858879	0.00201	0.00198
0.025	2.9832858	2.9832858	2.9835218	0.00791	0.00791
0.05	2.9731941	2.9731942	2.9741273	0.03138	0.03137
0.1	2.9340570	2.9340576	2.9376272	0.12153	0.12151

The dimensionless critical buckling load is compared to the results of Simsek and Reddy [73] in Table 5 and the error percentage is determined.

$$(\overline{P_{cr}} = P_{cr}\frac{L^2}{EI})$$

Table 5. The nondimensional critical buckling load of a sandwich nanocomposite beam

L/H	Simsek and Reddy [73] (TSDBT)	present study	Error %
20	9.8059	9.8066	0.007

5. Results and discussion

In this article, the behavior of deflection, buckling and vibration of a five-layer sandwich nanocomposite beam with foam core reinforced with GPLs and SMAs, is expressed for various parameters such as modes, aspect ratio, thickness ratio, layer arrangement and fibers angles. Also, the effect of adding GPLs, SMAs and their different volume fractions is investigated on the behavior of the beam. The parameters including mode, geometry of beam, applied forces, fibers angles and volume fraction of the materials are shown in Table 6.

Table 6. Values of mode, geometry of beam, applied forces, fibers angles and volume fraction of GPLs, SMAs and resin in GPLs-containing face sheets

$m=1$
$H=6\ \text{cm}$ $H_C=3\ \text{cm}$
$H_{(m)}=0\ \text{N}$ $q_{(m)}=-10000\ \frac{\text{N}}{\text{m}^2}$
$\text{fibers angles}=[0^\circ\ \ 30^\circ\ \ 45^\circ\ \ 60^\circ\ \ 90^\circ]$
$V_{GPL}=0.03 \xrightarrow{\text{According to table 1}} \eta_1=2.929\ \ \eta_2=2.855\ \ \eta_3=11.842$ $V_m\,(\text{in GPL layers})=0.5$ $V_{SMA}=0.01$

As it is shown in Fig 2-a, with the increase of L/H value due to the increase of the [K]-1 matrix and according to the Eq. (19), the deflection of the beam increases. These changes are more intense for higher H_C/H ratio and as the core thickness increases due to the low modulus of elasticity, the equivalent stiffness of the beam decreases and as a result, the beam becomes more flexible.

In Fig 2-b, as the value of L/H increases, the two matrices [K] and [M] decrease, but due to the further decrease of the matrix [K] and according to the Eq. (20), the first natural frequency of beam vibration decreases. Also, as the thickness of the core increases, the first natural frequency value of the beam decreases due to the reduction of the equivalent stiffness of the beam.

In Fig 2-c, the critical buckling load is higher at lower ratio of H_C/H due to the smaller thickness of the core and having a higher equivalent stiffness. Also, by increasing the value of L/H due to the reduction of [K] and [K_P] matrices and according to the Eq. (21), the critical buckling load also decreases and buckling occurs earlier.

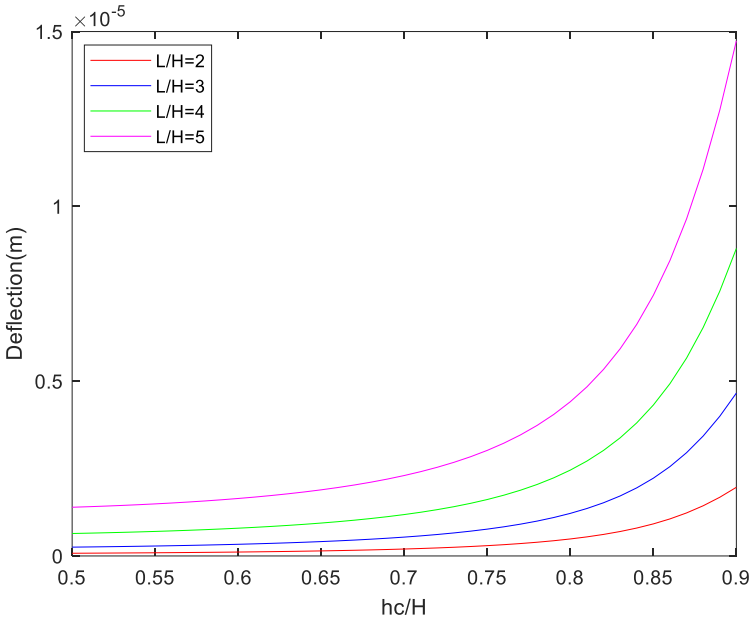
×10^-5
1.5
1
0.5
0
Deflection(m)
L/H=2
L/H=3
L/H=4
L/H=5
0.5
0.55
0.6
0.65
0.7
0.75
0.8
0.85
0.9
hc/H

(a)

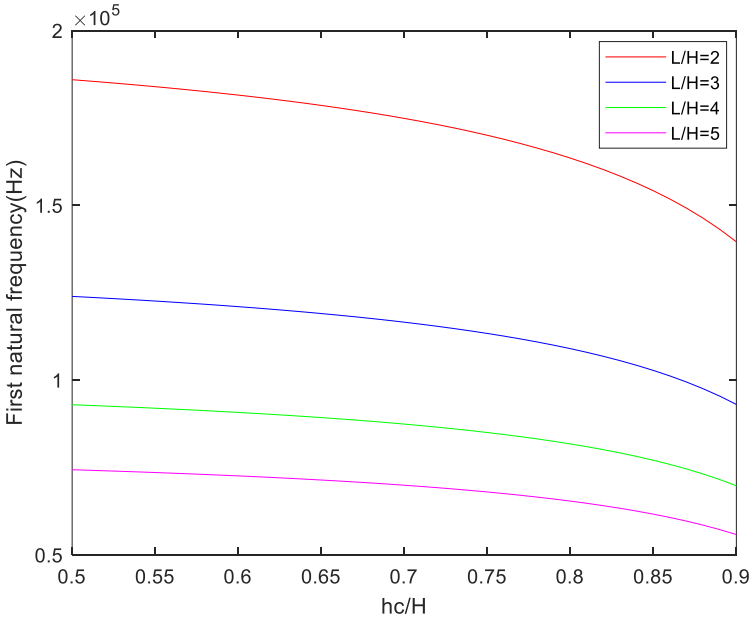
×10^5
2
1.5
1
0.5
First natural frequency(Hz)
L/H=2
L/H=3
L/H=4
L/H=5
0.5
0.55
0.6
0.65
0.7
0.75
0.8
0.85
0.9
hc/H

(b)

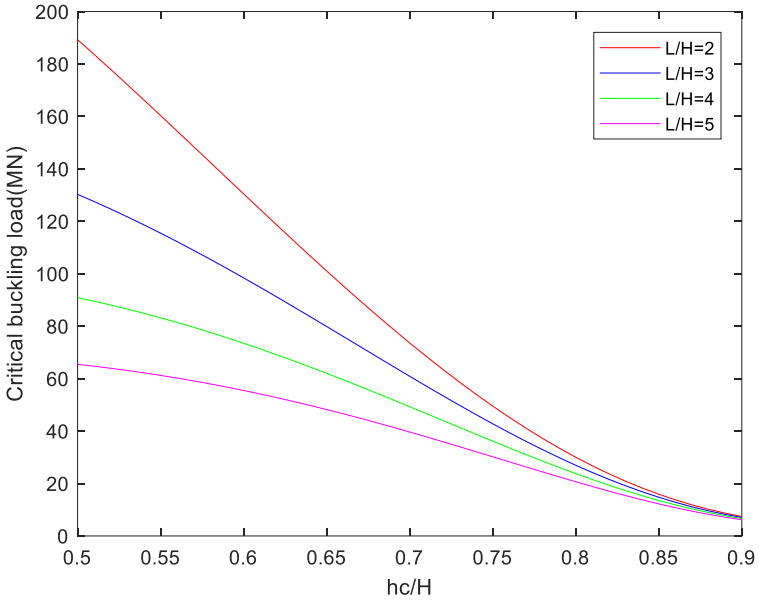

(c)

Fig 2. The effect of length-to-thickness ratio and core thickness-to-beam thickness ratio on (a) deflection, (b) first natural frequency and (c) critical buckling load of the beam

It is obvious in Fig. 3 that the behavior of the reinforced beam with GPLs improves in compared to the non-reinforced beam. It is also evident that increasing the volume fraction of GPL reinforcements increases the equivalent modulus and consequently the equivalent stiffness of the beam due to its high elasticity modulus. Therefore, the deflection decreases and frequency and the buckling load of the beam increases.

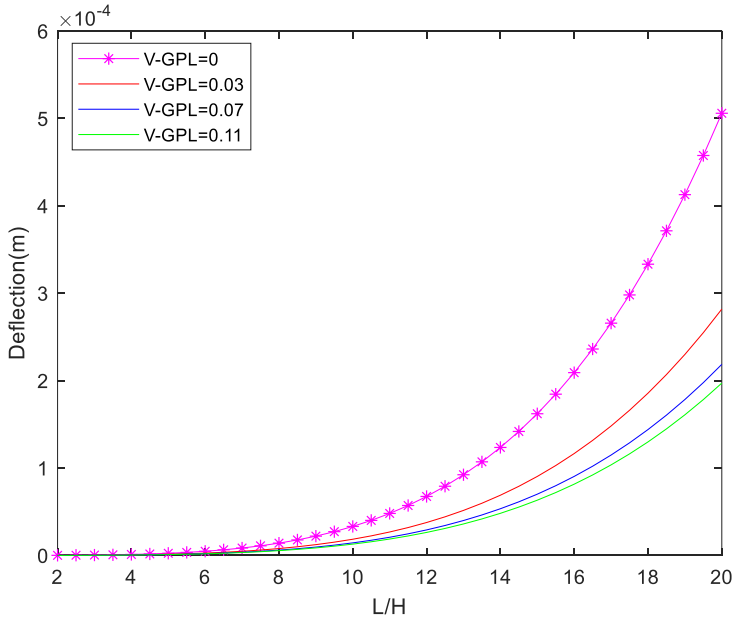

(a)

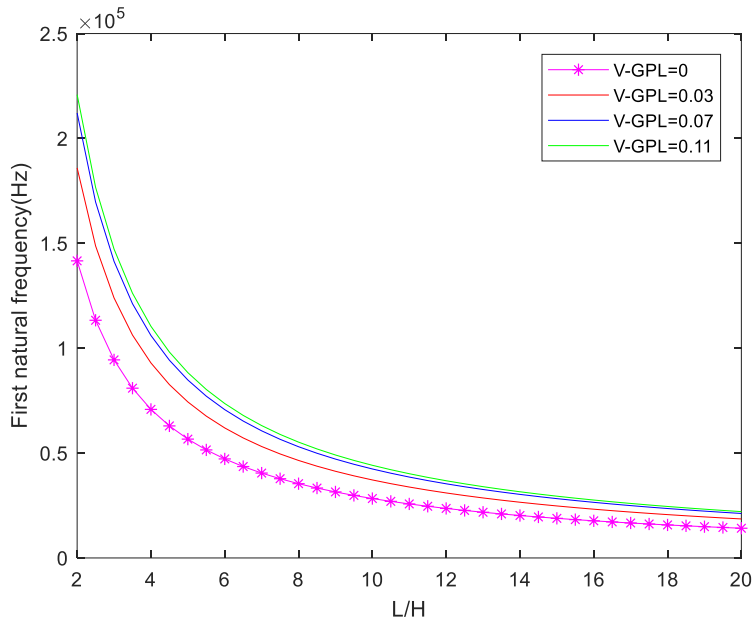

(b)

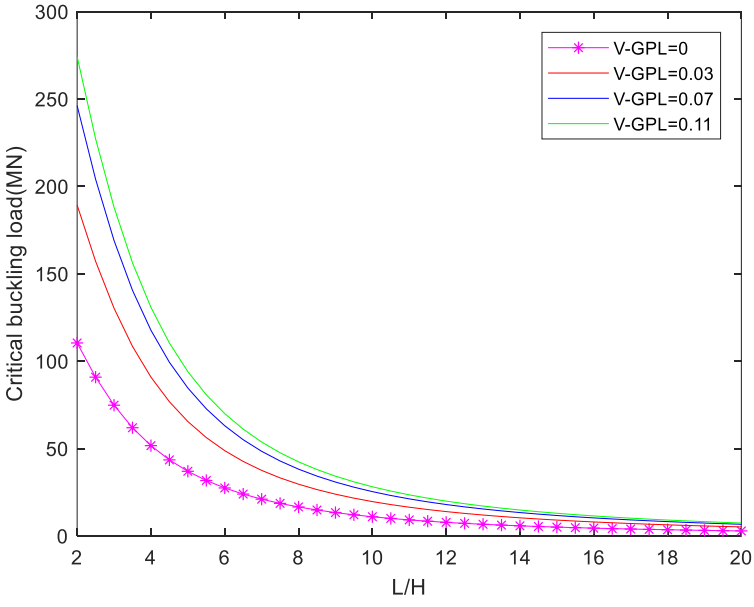

(c)

Fig 3. The effect of volume fraction of GPL on (a) deflection, (b) frequency and (c) buckling load

As shown in Fig. 4, the effect of adding SMAs in the beam is a little effect due to the lack of temperature changes in the problem and considering only the martensite phase of SMAs, which has a low elastic modulus. Therefore, different volume fractions of SMAs do not cause significant changes in deflection and buckling load of the beam. It also has a negative effect on frequency of the beam, and with the increase in the volume fraction of SMAs due to high density, the [M] matrix increases and according to equation (20), frequency of the beam decreases slightly.

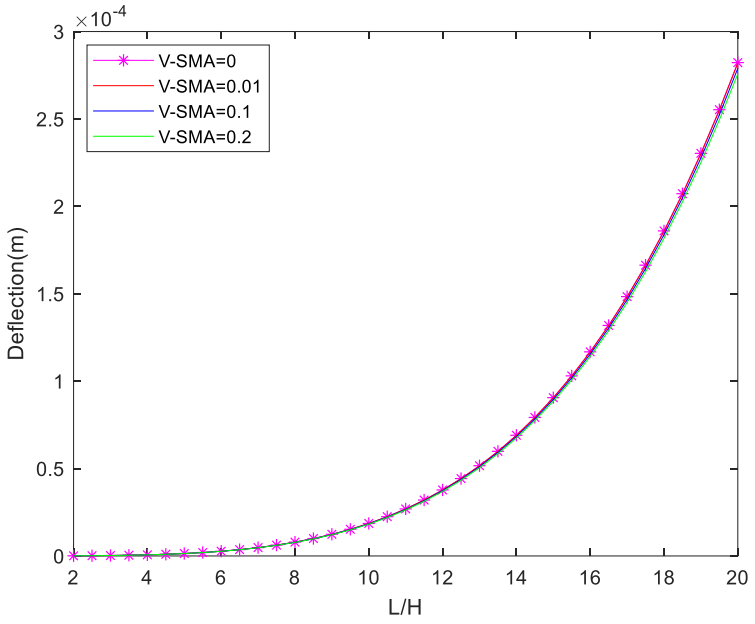
×10^-4
V-SMA=0
V-SMA=0.01
V-SMA=0.1
V-SMA=0.2
Deflection(m)
L/H

(a)

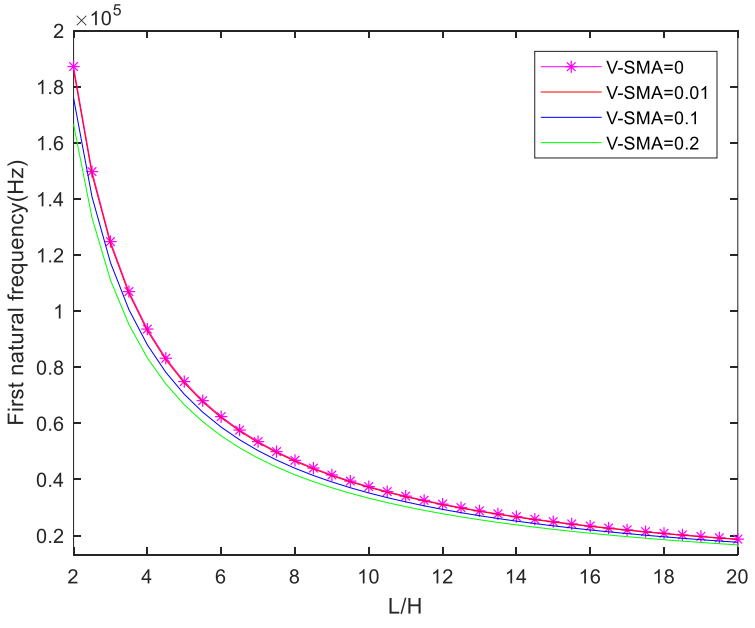
×10^5
V-SMA=0
V-SMA=0.01
V-SMA=0.1
V-SMA=0.2
First natural frequency(Hz)
L/H

(b)

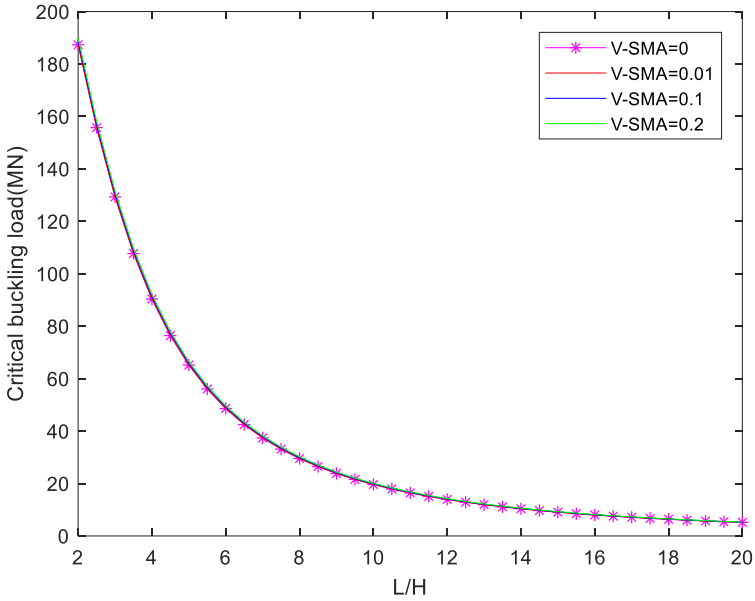

(c)

Fig 4. The effect of volume fraction of SMA on (a) deflection, (b) first natural frequency and (c) critical buckling load of the beam

In Tables 7 and 8, the analytical results of deflection, first natural frequency and critical buckling load of a sandwich nanocomposite beam determine according to the ratio of length to thickness of the beam, arrangement of layers and different fibers angles.

Table 7. Values of deflection, first natural frequency and critical buckling load of sandwich nanocomposite beam according to different fiber arrangement and angles

fibers angles (degree)	L/H	Deflection (m)	first natural frequency (Hz)	critical buckling load (N)
[0 30 45 60 90]	2	7.7079e-08	1.8594e+05	1.8929e+08
	3	2.5199e-07	1.2396e+05	1.3027e+08
	4	6.4220e-07	9.2969e+04	9.0876e+07
	5	1.3930e-06	7.4375e+04	6.5460e+07
[90 60 45 30 0]	2	6.8403e-08	1.8594e+05	2.1330e+08
	3	2.1664e-07	1.2396e+05	1.5153e+08
	4	5.4038e-07	9.2969e+04	1.0800e+08
	5	1.1558e-06	7.4375e+04	7.8895e+07
[0 45 0 45 0]	2	7.0647e-08	2.1898e+05	2.0652e+08
	3	2.1072e-07	1.4599e+05	1.5579e+08
	4	5.0170e-07	1.0949e+05	1.1633e+08
	5	1.0385e-06	8.7593e+04	8.7812e+07
[45 0 45 0 45]	2	6.4320e-08	2.0580e+05	2.2684e+08
	3	2.0269e-07	1.3720e+05	1.6196e+08
	4	5.0361e-07	1.0290e+05	1.1588e+08
	5	1.0743e-06	8.2319e+04	8.4885e+07
[0 30 90 30 0]	2	7.7224e-08	2.1073e+05	1.8893e+08
	3	2.2940e-07	1.4049e+05	1.4310e+08
	4	5.4422e-07	1.0536e+05	1.0724e+08
	5	1.1235e-06	8.4291e+04	8.1169e+07
[90 30 0 30 90]	2	8.2760e-08	1.8958e+05	1.7630e+08
	3	2.5433e-07	1.2639e+05	1.2908e+08
	4	6.2012e-07	9.4792e+04	9.4112e+07
	5	1.3057e-06	7.5833e+04	9.4112e+07

[30 60 0 60 30]	2	6.6014e-08	1.9524e+05	2.2102e+08
	3	2.1228e-07	1.3016e+05	1.5464e+08
	4	5.3504e-07	9.7622e+04	1.0908e+08
	5	1.1523e-06	7.8098e+04	7.9139e+07
[60 45 90 45 60]	2	7.3123e-08	1.5729e+05	1.9953e+08
	3	2.5911e-07	1.0486e+05	1.2669e+08
	4	6.9540e-07	7.8644e+04	8.3924e+07
	5	1.5579e-06	6.2915e+04	5.8534e+07
[60 90 0 90 60]	2	8.7877e-08	1.6576e+05	1.6603e+08
	3	2.8443e-07	1.1051e+05	1.1542e+08
	4	7.2008e-07	8.2882e+04	8.1048e+07
	5	1.5553e-06	6.6306e+04	5.8632e+07
[30 45 60 45 30]	2	6.0631e-08	1.8518e+05	2.4064e+08
	3	2.0634e-07	1.2346e+05	1.5910e+08
	4	5.4015e-07	9.2592e+04	1.0805e+08
	5	1.1919e-06	7.4073e+04	7.6507e+07

Table 8. The effect of specific angle of laminate in face sheet layers

fibers angles (degree)	L/H	Deflection (m)	first natural frequency (Hz)	critical buckling load (N)
[0 0 0 0 0]	2	1.0161e-07	2.4322e+05	1.4359e+08
	3	2.7308e-07	1.6215e+05	1.2021e+08
	4	5.9101e-07	1.2161e+05	9.8747e+07
	5	1.1332e-06	9.7288e+04	8.0469e+07
[45 45 45 45 45]	2	5.9766e-08	1.7649e+05	2.4412e+08
	3	2.1104e-07	1.1766e+05	1.5555e+08
	4	5.6525e-07	8.8247e+04	1.0325e+08
	5	1.2648e-06	7.0597e+04	7.2097e+07
[90 90 90 90 90]	2	1.2990e-07	1.2975e+05	1.1232e+08
	3	4.2607e-07	8.6500e+04	7.7049e+07
	4	1.0880e-06	6.4875e+04	5.3640e+07
	5	2.3630e-06	5.1900e+04	3.8590e+07

In Fig. 5 and Table 9, the results of buckling load and frequency for a sandwich nanocomposite beam define according to the first three modes and length to thickness ratio of the beam. It is concluded that in higher modes, the buckling and frequency increase.

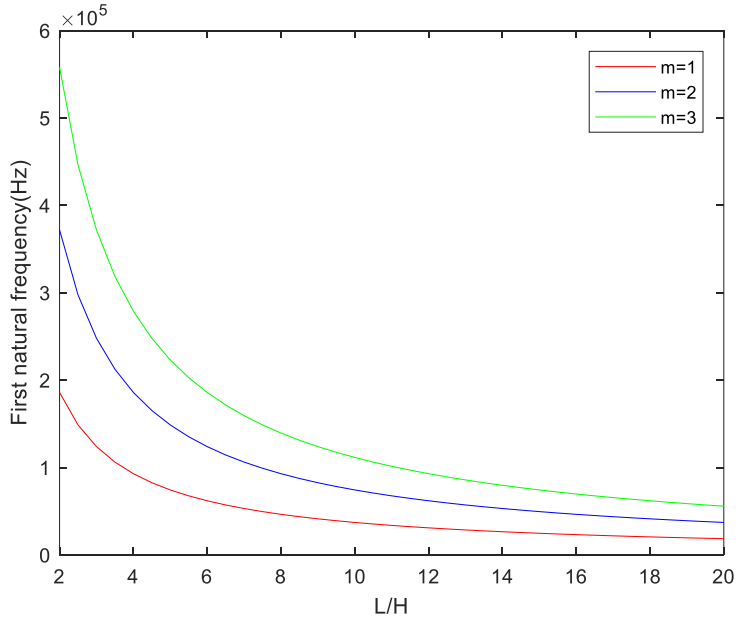

(a)

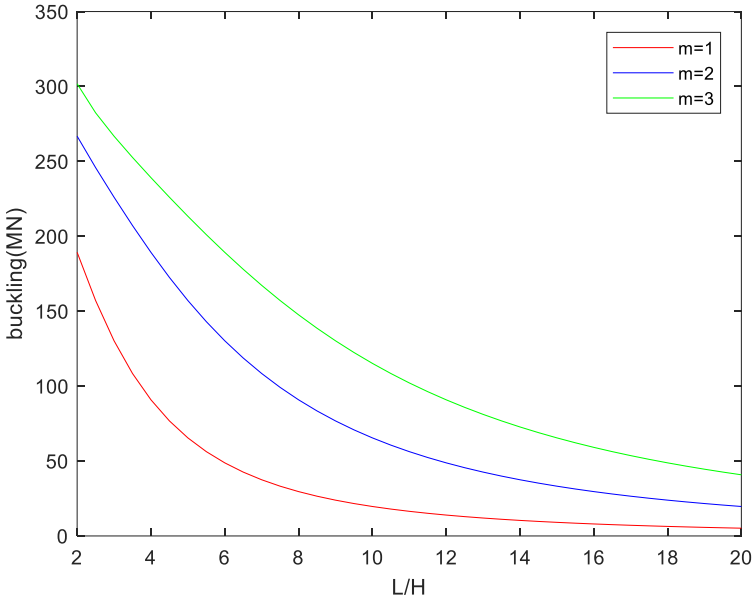

(b)

Fig 5. The effect of mode on (a) frequency and (b) buckling load

Table 9. Values of deflection, frequency and buckling load of sandwich nanocomposite beam according to different modes

mode	L/H	first natural frequency (Hz)	critical buckling load (N)
1	2	1.859e+05	1.893e+08
	3	1.24e+05	1.303e+08
	4	9.297e+04	9.088e+07
	5	7.438e+04	6.546e+07
2	2	3.719e+05	2.668e+08
	3	2.479e+05	2.261e+08
	4	1.859e+05	1.893e+08
	5	1.488e+05	1.571e+08
3	2	5.578e+05	3.018e+08
	3	3.719e+05	2.668e+08
	4	2.789e+05	2.392e+08
	5	2.231e+05	2.134e+08

Fig. 6 shows that the employing fibers in the face sheets of the core increases the stiffness and equivalent modulus of elasticity of the structure, so the deflection decreases and the first natural frequency and critical buckling load of the beam increase.

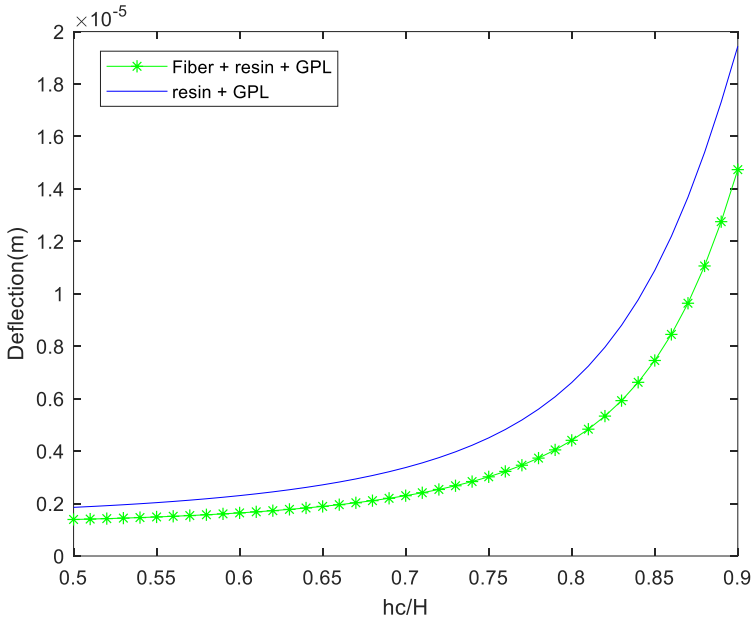

(a)

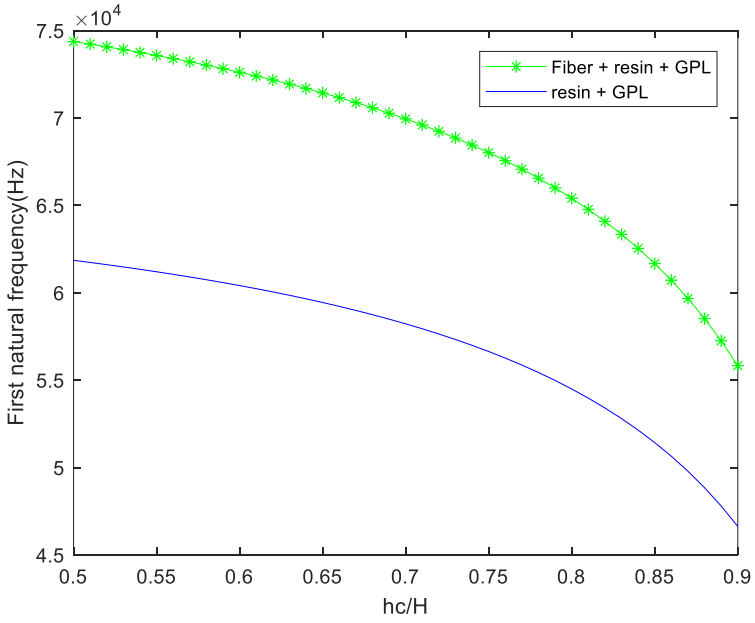

(b)

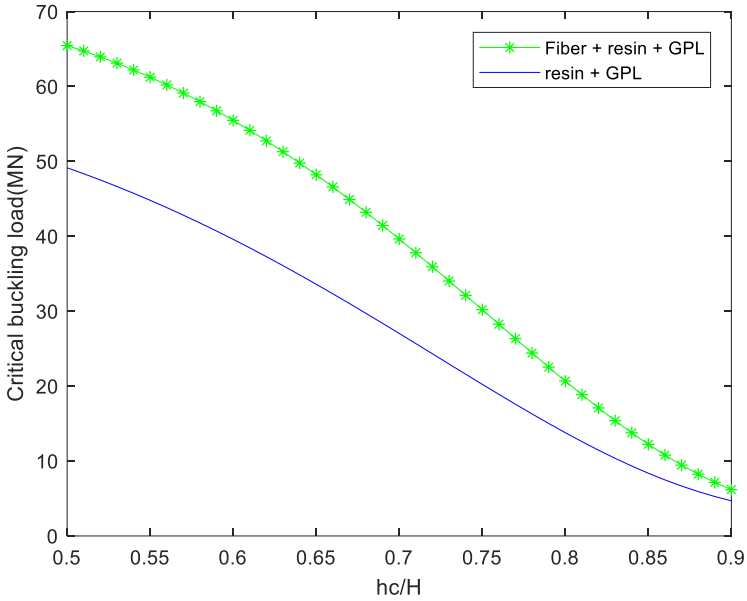

(c)

Fig 6. The effect of employing fiber on (a) deflection, (b) first natural frequency and (c) critical buckling load for the sandwich beam

6. Conclusion

In the present study, the governing equations of motion for the five-layer nanocomposite sandwich beam with foam core, reinforced with GPLs and SMAs, are derived based on TSDBT. The analytical results for deflection, critical buckling load and natural frequencies of beam are obtained. Also, the equivalent mechanical properties of the layers are extracted from the extended mixture rule. The analytical results are mentioned based on different parameters which stated as follows:

- By increasing aspect ratio (L/H) ratio, the deflection of the beam increases and the natural frequencies and the critical buckling load decrease.
- Using a light core like foam in the beam structure reduces the overall weight and density of the structure, and its high thickness increases the flexural stiffness. As a result, it provides a high strength-to-weight ratio for the beam.
- As mentioned before, with the increase of the H_C/H ratio, due to the low Young's modulus of the core, the equivalent modulus of the structure decreases, so the deflection of the beam increases and the natural frequencies and critical buckling load decrease.
- The effect of adding reinforcements to the matrix is very impressive and practical due to their high Young's modulus. As mentioned, mixing a small amount of GPLs in the polymer matrix provides a high equivalent stiffness for the structure. By adding only 0.03 volume fraction of GPL, the deflection of the beam decrease by 44% and the critical buckling load and first natural frequency increases by 79% and 31%, respectively.
- The influence of SMAs is significant when their thermal performance is considered. In this study, due to the lack of temperature changes, the addition of SMAs in the polymer matrix does not change the equivalent stiffness of the beam greatly, so it does not have a large effect on the deflection, the critical buckling load of the beam. Also, due to the high density of SMAs, it has the opposite effect on the natural frequencies and causes them to decrease.
- The effect of employing fibers in face sheet layers for the sandwich structure leads to decrease the deflection and increase the natural frequency and the critical buckling load. It is concluded that the used fibers as well as GPL reinforcements increases the stiffness and equivalent modulus of elasticity of the structure.

Declaration of conflicting interests

The author(s) declared no potential conflicts of interest with respect to the research, authorship, and/or publication of this article.

Nomenclature:

E	modulus of elasticity
G	shear modulus
υ	poisson's ratio
ρ	density
m	mod
L	length
H	height
l	Length of GPL
h	thickness of GPL
w	width of GPL
η	efficiency parameter
V	volume fraction
$U_{(x,y,z,t)}$	axial displacements
$u_{(x,t)}$	axial displacements at the middle plane
$V_{(x,y,z,t)}$	axial displacements
$W_{(x,y,z,t)}$	transverse displacements
$w_{(x,t)}$	transverse displacements at the middle plane
ψ	rotation of the cross section
U	strain energy
W_{ext}	external energy
T	kinetic energy
$H_{(x)}$	longitudinal load
$q_{(x)}$	transverse load
P_{cr}	critical buckling load

Acknowledgement

The authors would like to thank the referees for their valuable comments and also thanks a lot to increase the quality of the present work. The author(s) disclosed receipt of the following financial support for the research, authorship, and/or publication of this article.

References:

[1] A. Mihankhah, Z. K. Maraghi, A. G. Arani, S. Niknejad, Vibrations of Multi-Layer Beam with Nanocomposite Face Sheets Reinforced with Graphene Platelets and Porous Core, *Journal of Solid Mechanics*, Vol. 15, No. 3, 2023.

[2] M. Hosseinkhani, H. Ghavami, M. Haghighi-Yazdi, M. Mosavi Mashhadi, M. Safarabadi, Investigation of viscoelastic properties in composite sandwich panels subjected to low-velocity impact: Experimental and numerical approaches, *Journal of Sandwich Structures & Materials*, Vol. 25, No. 4, pp. 478-498, 2023.

[3] H. Sun, H. Yuan, J. Zhang, J. Zhang, J. Du, W. Huang, Dynamic response of multilayer sandwich beams with foam-filled trapezoidal corrugated and foam cores under low-velocity impact, *Engineering Structures*, Vol. 286, pp. 116080, 2023.

[4] F. Bargozini, M. Mohammadimehr, The theoretical and experimental buckling analysis of a nanocomposite beams reinforced by nanorods made of recycled materials, *Polymer Composites*, Vol. 45, No. 4, pp. 3327-3342, 2024.

[5] K. Zhu, X. Zheng, C. Zhang, J. Peng, D. Zhang, L. Yan, The behavior of interlocked ortho-grid composite sandwich structure subjected to low-velocity impact, *Composite Structures*, Vol. 304, pp. 116399, 2023.

[6] H. Lv, S. Shi, B. Chen, J. Ma, Z. Sun, Low-velocity impact response of composite sandwich structure with grid–honeycomb hybrid core, *International Journal of Mechanical Sciences*, Vol. 246, pp. 108149, 2023.

[7] F. Bargozini, M. Mohammadimehr, E. A. Dawi, M. Salavati-Niasari, Buckling of a sandwich beam with carbon nano rod reinforced composite and porous core under axially variable forces by considering general strain, *Results in Engineering*, pp. 101945, 2024.

[8] C. Zheng, P. Sun, Y. Fu, X. Fu, Q. Li, Structural optimization to improve the dynamic performance of novel co-curing damping sandwich composites, *Polymer Composites*, Vol. 44, No. 4, pp. 2474-2487, 2023.

[9] K. Falkowicz, Experimental and numerical failure analysis of thin-walled composite plates using progressive failure analysis, *Composite Structures*, Vol. 305, pp. 116474, 2023.

[10] M. Emdadi, M. Mohammadimehr, F. Bargozini, Vibration of a Nanocomposite Annular Sandwich Microplate Based on HSDT Using DQM, *Multiscale Science and Engineering*, pp. 1-15, 2024.

[11] M. Khosravi, S. J. Mehrabadi, K. M. Fard, Vibration Behavior of Thick Sandwich Composite Beam with Flexible Core Resting on Incompressible Fluid Foundation, *Journal of Solid Mechanics*, Vol. 15, No. 1, 2023.

[12] M. Emdadi, M. Mohammadimehr, Dynamic stability of the double-bonded annular nanocomposite sandwich microplate on viscoelastic foundation, *Journal of Sandwich Structures & Materials*, Vol. 24, No. 1, pp. 385-418, 2022.

[13] V. Kallannavar, S. Kattimani, B. Reddy, Influence of temperature on the vibration control of the laminated composite sandwich plate with a 3D printed PLA core, in *Proceeding of*, AIP Publishing, pp.

[14] M. A. Hamed, R. M. Abo-Bakr, S. A. Mohamed, M. A. Eltaher, Influence of axial load function and optimization on static stability of sandwich functionally graded beams with porous core, *Engineering with Computers*, Vol. 36, pp. 1929-1946, 2020.

[15] A. A. Monajemi, M. Mohammadimehr, Stability analysis of a spinning soft-core sandwich beam with CNTs reinforced metal matrix nanocomposite skins subjected to residual stress, *Mechanics Based Design of Structures and Machines*, Vol. 52, No. 1, pp. 338-358, 2024.

[16] M. Charekhli-Inanllo, M. Mohammadimehr, The effect of various shape core materials by FDM on low velocity impact behavior of a sandwich composite plate, *Engineering Structures*, Vol. 294, pp. 116721, 2023.

[17] A. Farazin, M. Mohammadimehr, Nano research for investigating the effect of SWCNTs dimensions on the properties of the simulated nanocomposites: a molecular dynamics simulation, *Advances in nano research*, Vol. 9, No. 2, pp. 83-90, 2020.

[18] M. Bouazza, A. M. Zenkour, Vibration of inhomogeneous fibrous laminated plates using an efficient and simple polynomial refined theory, *Journal of Computational Applied Mechanics*, Vol. 52, No. 2, pp. 233-245, 2021.

[19] R. Hosseini, M. Babaei, A. Nadaf Oskouei, A review on structural response and energy absorption of sandwich structures with 3D printed core, *Journal of Computational Applied Mechanics*, Vol. 54, No. 4, pp. 623-644, 2023.

[20] F. Bargozini, M. Mohammadimehr, E. A. Dawi, R. Monsef, Z. Heydariyan, M. Salavati-Niasari, Development and performance analysis of a 316 stainless steel autoclave for facile fabrication of carbon nanoarchitectures derived from natural potato and starch, *Journal of Materials Research and Technology*, Vol. 23, pp. 3126-3136, 2023.

[21] S. Shahedi, M. Mohammadimehr, Vibration analysis of rotating fully-bonded and delaminated sandwich beam with CNTRC face sheets and AL-foam flexible core in thermal and moisture environments, *Mechanics Based Design of Structures and Machines*, Vol. 48, No. 5, pp. 584-614, 2020.

[22] A. Tamrabet, C. Mourad, N. Ali Alselami, A. Menasria, B. Mamen, A. Bouhadra, Efficient Kinematic model for Stability Analysis of Imperfect Functionally Graded Sandwich Plates with Ceramic middle layer and Varied Boundary Edges, *Journal of Computational Applied Mechanics*, 2024.

[23] R. Hosseini, M. Babaei, A. Naddaf Oskouei, The influences of various auxetic cores on natural frequencies and forced vibration behavior of sandwich beam fabricated by 3D printer based on third-order shear deformation theory, *Journal of Computational Applied Mechanics*, Vol. 54, No. 2, pp. 285-308, 2023.

[24] M. Kazemi, Experimental analysis of sandwich composite beams under three-point bending with an emphasis on the layering effects of foam core, in *Proceeding of*, Elsevier, pp. 383-391.

[25] A. A. Nia, M. Kazemi, Experimental study of ballistic resistance of sandwich targets with aluminum face-sheet and graded foam core, *Journal of Sandwich Structures & Materials*, Vol. 22, No. 2, pp. 461-479, 2020.

[26] Q. H. Qin, T. J. Wang, An analytical solution for the large deflections of a slender sandwich beam with a metallic foam core under transverse loading by a flat punch, *Composite Structures*, Vol. 88, No. 4, pp. 509-518, 2009.

[27] J. Zhang, Q. Qin, T. J. Wang, Compressive strengths and dynamic response of corrugated metal sandwich plates with unfilled and foam-filled sinusoidal plate cores, *Acta Mechanica*, Vol. 224, No. 4, pp. 759-775, 2013.

[28] R. Nasirzadeh, A. R. Sabet, Study of foam density variations in composite sandwich panels under high velocity impact loading, *International Journal of Impact Engineering*, Vol. 63, pp. 129-139, 2014.

[29] C. Feng, S. Kitipornchai, J. Yang, Nonlinear free vibration of functionally graded polymer composite beams reinforced with graphene nanoplatelets (GPLs), *Engineering Structures*, Vol. 140, pp. 110-119, 2017.

[30] Y. Wang, C. Feng, X. Wang, Z. Zhao, C. S. Romero, Y. Dong, J. Yang, Nonlinear static and dynamic responses of graphene platelets reinforced composite beam with dielectric permittivity, *Applied Mathematical Modelling*, Vol. 71, pp. 298-315, 2019.

[31] M. Mohammadi, M. Goodarzi, M. Ghayour, A. Farajpour, Influence of in-plane pre-load on the vibration frequency of circular graphene sheet via nonlocal continuum theory, *Composites Part B: Engineering*, Vol. 51, pp. 121-129, 2013.

[32] R. M. R. Reddy, W. Karunasena, W. Lokuge, Free vibration of functionally graded-GPL reinforced composite plates with different boundary conditions, *Aerospace Science and Technology*, Vol. 78, pp. 147-156, 2018.

[33] H. Wu, J. Yang, S. Kitipornchai, Dynamic instability of functionally graded multilayer graphene nanocomposite beams in thermal environment, *Composite Structures*, Vol. 162, pp. 244-254, 2017.

[34] Y. Kiani, M. Mirzaei, Enhancement of non-linear thermal stability of temperature dependent laminated beams with graphene reinforcements, *Composite Structures*, Vol. 186, pp. 114-122, 2018.

[35] M. Mohammadi, A. Farajpour, A. Moradi, M. Ghayour, Shear buckling of orthotropic rectangular graphene sheet embedded in an elastic medium in thermal environment, *Composites Part B: Engineering*, Vol. 56, pp. 629-637, 2014.

[36] M. Song, Y. Gong, J. Yang, W. Zhu, S. Kitipornchai, Nonlinear free vibration of cracked functionally graded graphene platelet-reinforced nanocomposite beams in thermal environments, *Journal of Sound and Vibration*, Vol. 468, pp. 115115, 2020.

[37] C. Feng, S. Kitipornchai, J. Yang, Nonlinear bending of polymer nanocomposite beams reinforced with non-uniformly distributed graphene platelets (GPLs), *Composites Part B: Engineering*, Vol. 110, pp. 132-140, 2017.

[38] J. Yang, H. Wu, S. Kitipornchai, Buckling and postbuckling of functionally graded multilayer graphene platelet-reinforced composite beams, *Composite Structures*, Vol. 161, pp. 111-118, 2017.

[39] Y. Wang, K. Xie, T. Fu, C. Shi, Vibration response of a functionally graded graphene nanoplatelet reinforced composite beam under two successive moving masses, *Composite structures*, Vol. 209, pp. 928-939, 2019.

[40] M. Mohammadi, A. Moradi, M. Ghayour, A. Farajpour, Exact solution for thermo-mechanical vibration of orthotropic mono-layer graphene sheet embedded in an elastic medium, *Latin American Journal of Solids and Structures*, Vol. 11, pp. 437-458, 2014.

[41] M. Song, J. Yang, S. Kitipornchai, Bending and buckling analyses of functionally graded polymer composite plates reinforced with graphene nanoplatelets, *Composites Part B: Engineering*, Vol. 134, pp. 106-113, 2018.

[42] Z. Yang, M. Tam, Y. Zhang, S. Kitipornchai, J. Lv, J. Yang, Nonlinear dynamic response of FG graphene platelets reinforced composite beam with edge cracks in thermal environment, *International Journal of Structural stability and dynamics*, Vol. 20, No. 14, pp. 2043005, 2020.

[43] K. Majidi-Mozafari, R. Bahaadini, A. R. Saidi, R. Khodabakhsh, An analytical solution for vibration analysis of sandwich plates reinforced with graphene nanoplatelets, *Engineering with Computers*, pp. 1-17, 2022.

[44] M. Mohammadi, A. Farajpour, M. Goodarzi, F. Dinari, Thermo-mechanical vibration analysis of annular and circular graphene sheet embedded in an elastic medium, *Latin American Journal of Solids and Structures*, Vol. 11, pp. 659-682, 2014.

[45] J. J. Lee, S. Choi, Thermal buckling and postbuckling analysis of a laminated composite beam with embedded SMA actuators, *Composite Structures*, Vol. 47, No. 1-4, pp. 695-703, 1999.

[46] M. M. Barzegari, M. Dardel, A. Fathi, Vibration analysis of a beam with embedded shape memory alloy wires, *Acta Mechanica Solida Sinica*, Vol. 26, No. 5, pp. 536-550, 2013.

[47] L.-C. Shiau, S.-Y. Kuo, S.-Y. Chang, Free vibration of buckled SMA reinforced composite laminates, *Composite Structures*, Vol. 93, No. 11, pp. 2678-2684, 2011.

[48] J.-S. Park, J.-H. Kim, S.-H. Moon, Vibration of thermally post-buckled composite plates embedded with shape memory alloy fibers, *Composite structures*, Vol. 63, No. 2, pp. 179-188, 2004.

[49] S. Kamarian, M. Bodaghi, R. B. Isfahani, J.-i. Song, A comparison between the effects of shape memory alloys and carbon nanotubes on the thermal buckling of laminated composite beams, *Mechanics Based Design of Structures and Machines*, Vol. 50, No. 7, pp. 2250-2273, 2022.

[50] R. K. Mahabadi, M. Shakeri, M. D. Pazhooh, Free vibration of laminated composite plate with shape memory alloy fibers, *Latin American Journal of Solids and Structures*, Vol. 13, pp. 314-330, 2016.

[51] H. Asadi, M. Bodaghi, M. Shakeri, M. M. Aghdam, On the free vibration of thermally pre/post-buckled shear deformable SMA hybrid composite beams, *Aerospace Science and Technology*, Vol. 31, No. 1, pp. 73-86, 2013.

[52] H. Asadi, M. Bodaghi, M. Shakeri, M. M. Aghdam, Nonlinear dynamics of SMA-fiber-reinforced composite beams subjected to a primary/secondary-resonance excitation, *Acta Mechanica*, Vol. 226, pp. 437-455, 2015.

[53] H.-S. Shen, Y. Xiang, F. Lin, Nonlinear bending of functionally graded graphene-reinforced composite laminated plates resting on elastic foundations in thermal environments, *Composite Structures*, Vol. 170, pp. 80-90, 2017.

[54] Ö. Civalek, Ş. D. Akbaş, B. Akgöz, S. Dastjerdi, Forced vibration analysis of composite beams reinforced by carbon nanotubes, *Nanomaterials*, Vol. 11, No. 3, pp. 571, 2021.

[55] H.-S. Shen, C. Li, Modeling and Re-Examination of Nonlinear Vibration and Nonlinear Bending of Sandwich Plates with Porous FG-GPLRC Core, *Advanced Engineering Materials*, Vol. 25, No. 13, pp. 2300299, 2023.

[56] M. Anvari, M. Mohammadimehr, A. Amiri, Vibration behavior of a micro cylindrical sandwich panel reinforced by graphene platelet, *Journal of Vibration and Control*, Vol. 26, No. 13-14, pp. 1311-1343, 2020.

[57] A. Amiri, M. Mohammadimehr, M. I. Rahaghi, Vibration analysis of a micro-cylindrical sandwich panel with reinforced shape-memory alloys face sheets and porous core, *The European Physical Journal Plus*, Vol. 136, No. 8, pp. 887, 2021.

[58] S. M. AkhavanAlavi, M. Mohammadimehr, S. H. Edjtahed, Active control of micro Reddy beam integrated with functionally graded nanocomposite sensor and actuator based on linear quadratic regulator method, *European Journal of Mechanics-A/Solids*, Vol. 74, pp. 449-461, 2019.

[59] B. Akgöz, Ö. Civalek, Vibrational characteristics of embedded microbeams lying on a two-parameter elastic foundation in thermal environment, *Composites Part B: Engineering*, Vol. 150, pp. 68-77, 2018.

[60] Ö. Civalek, S. Dastjerdi, B. Akgöz, Buckling and free vibrations of CNT-reinforced cross-ply laminated composite plates, *Mechanics Based Design of Structures and Machines*, Vol. 50, No. 6, pp. 1914-1931, 2022.

[61] N. Adab, M. Arefi, Vibrational behavior of truncated conical porous GPL-reinforced sandwich micro/nano-shells, *Engineering with Computers*, Vol. 39, No. 1, pp. 419-443, 2023.

[62] M. Mohammadi, A. Farajpour, M. Goodarzi, Numerical study of the effect of shear in-plane load on the vibration analysis of graphene sheet embedded in an elastic medium, *Computational Materials Science*, Vol. 82, pp. 510-520, 2014.

[63] M. Avcar, L. Hadji, Ö. Civalek, Natural frequency analysis of sigmoid functionally graded sandwich beams in the framework of high order shear deformation theory, *Composite structures*, Vol. 276, pp. 114564, 2021.

[64] M. Mohammadi, M. Hosseini, M. Shishesaz, A. Hadi, A. Rastgoo, Primary and secondary resonance analysis of porous functionally graded nanobeam resting on a nonlinear foundation subjected to mechanical and electrical loads, *European Journal of Mechanics-A/Solids*, Vol. 77, pp. 103793, 2019.

[65] H. Moosavi, M. Mohammadi, A. Farajpour, S. H. Shahidi, Vibration analysis of nanorings using nonlocal continuum mechanics and shear deformable ring theory, *Physica E: Low-dimensional Systems and Nanostructures*, Vol. 44, No. 1, pp. 135-140, 2011.

[66] M. Mohammadi, A. Farajpour, A. Moradi, M. Hosseini, Vibration analysis of the rotating multilayer piezoelectric Timoshenko nanobeam, *Engineering Analysis with Boundary Elements*, Vol. 145, pp. 117-131, 2022/12/01/, 2022.

[67] M. Mohammadi, A. Farajpour, A. Rastgoo, Coriolis effects on the thermo-mechanical vibration analysis of the rotating multilayer piezoelectric nanobeam, *Acta Mechanica*, Vol. 234, No. 2, pp. 751-774, 2023/02/01, 2023.

[68] K. Alambeigi, M. Mohammadimehr, M. Bamdad, T. Rabczuk, Free and forced vibration analysis of a sandwich beam considering porous core and SMA hybrid composite face layers on Vlasov's foundation, *Acta Mechanica*, Vol. 231, pp. 3199-3218, 2020.

[69] L. Xin, Y. Kiani, Vibration characteristics of arbitrary thick sandwich beam with metal foam core resting on elastic medium, in *Proceeding of*, Elsevier, pp. 1-11.

[70] M. Mohammadi, M. Safarabadi, A. Rastgoo, A. Farajpour, Hygro-mechanical vibration analysis of a rotating viscoelastic nanobeam embedded in a visco-Pasternak elastic medium and in a nonlinear thermal environment, *Acta Mechanica*, Vol. 227, pp. 2207-2232, 2016.

[71] J. V. Santos, J. N. Reddy, Vibration of Timoshenko beams using non-classical elasticity theories, *Shock and Vibration*, Vol. 19, No. 3, pp. 251-256, 2012.

[72] G. R. Koochaki, Free vibration analysis of functionally graded beams, *World Academy of Science, Engineering and Technology*, Vol. 74, 2011.

[73] M. Şimşek, J. N. Reddy, A unified higher order beam theory for buckling of a functionally graded microbeam embedded in elastic medium using modified couple stress theory, *Composite Structures*, Vol. 101, pp. 47-58, 2013.